Inorg. Chem. **2007**, *46*, 8019–8023

Template-Free Fabrication of Hexagonal ZnO Microprism with an Interior Space

Shi-Yong Yu,[†,‡] Hong-Jie Zhang,*[,†] Ze-Ping Peng,[†,‡] Li-Ning Sun,[†,‡] and Wei-Dong Shi[†,‡]

Key Laboratory of Rare Earth Chemistry and Physics, Changchun Institute of Applied Chemistry, Chinese Academy of Sciences, Changchun 130022, P. R. China, and Graduate School of the Chinese Academy of Sciences, Beijing, P. R. China

Received May 9, 2007

Well-faceted hexagonal ZnO microprisms with regular interior space have been successfully prepared by a template-free hydrothermal synthetic route. The morphologies of the products depend on the experimental conditions such as the solvent, the concentration of ammonia aqueous solution, and the reaction temperature. Through manipulation of the aging time, the as-prepared ZnO can be controlled as a monodispersed hexagonal twinning solid or as hollow microprisms. Moreover, the evolution process of the hollow ZnO nanoarchitecture after reaction for 2, 6, 12, and 24 h has been investigated by field emission scanning electron microscopy (FE-SEM) and transmission electron microscopy (TEM). A possible growth mechanism has also been proposed and discussed. Furthermore, the photoluminescence (PL) measurement exhibits the unique emitting characteristic of hollow ZnO nanostructures.

Introduction

Hollow nanostructures with highly specific morphology and novel properties are of great interest to chemists and material scientists because of their unique properties and promising applications in material science and micro/nanodevices.[1−3] Moreover, as a result of requirement and rapid advancements in material science, hollow structures with novel morphology and nanoscale characteristics are demanded urgently. Until now, the general approach for fabricating hollow structures has involved the use of various removable or sacrificial templates.[4−6] Consequently, spherical hollow structures observed and obtained are still the most popular architecture because of their highest symmetry.[7−9] To overcome difficulties associated with the above template methods, such as material compatibility and process complexity, newer template-free methods under one-pot conditions are expectative for synthesizing desired nanomaterials. Controlled organization into a 1D nanostructure with interior space remains a challenge in nanoscale science, which is attractive to scientists not only because of its importance in understanding crystal growth of novel architectures but also for its promising application.[10−17]

ZnO is one of the most promising materials for optoelectronic applications owing to its wide band gap (3.37 eV) and large exciton binding energy (60 meV). Potential applications of nanostructured ZnO include light-emitting diodes,[18] room-temperature UV lasers,[19] solar cells,[20] and so

* To whom correspondence should be addressed. E-Mail: hongjie@ns.ciac.jl.cn. Tel: +86-431-85262127. Fax: +86-431-85698041.

[†] Changchun Institute of Applied Chemistry, Chinese Academy of Sciences.

[‡] Graduate School of the Chinese Academy of Sciences.

(1) Yin, Y. D.; Rioux, R. M.; Erdonmez, C. K.; Hughes, S.; Somorjai, G. A.; Alivisatos, A. P. *Science* **2004**, *304*, 711.
(2) Fan, H. J.; Knez, M.; Scholz, R.; Nielsch, K.; Pippel, E.; Hesse, D.; Zacharias, M.; Goesele, U. *Nat. Mater.* **2006**, *5*, 627.
(3) Hu, P.; Xiao, K.; Liu, Y. Q.; Yu, G.; Wang X.B.; Fu, L.; Cui, G. L.; Zhu, D. B. *Appl. Phys. Lett.* **2004**, *84*, 4932.
(4) Liang, Z. J.; Susha, A.; Caruso, F. *Chem. Mater.* **2003**, *15*, 3176.
(5) Wang, L.; Sasaki, T.; Ebina, Y.; Kurashima, K.; Watanabe, M. *Chem. Mater.* **2002**, *14*, 4827.
(6) Kanungo, M.; Deepa, P. N.; Collinson, M. M. *Chem. Mater.* **2004**, *16*, 5535.
(7) Dhas, N. A.; Suslick, K. S. *J. Am. Chem. Soc.* **2005**, *127*, 2368.
(8) Schmidt, H. T.; Gray, B. L.; Wingert, P. A.; Ostafin, A. E. *Chem. Mater.* **2004**, *16*, 4942.
(9) Fujiwara, M.; Shiokawa, K.; Tannaka, Y.; Nakahara, Y. *Chem. Mater.* **2004**, *16*, 5420.
(10) Wang, X.; Zhuang, J.; Peng, Q.; Li, Y. D. *Nature* **2005**, *437*, 121.
(11) Park, S.; Lim, J.-H.; Chung, S.-W.; Mirkin, C. A. *Science* **2004**, *303*, 348.
(12) Noble, P. F.; Cayre, O. J.; Alargova, R. G.; Velev, O. D.; Paunov, V. N. *J. Am. Chem. Soc.* **2004**, *126*, 8092.
(13) Dinsmore, A. D.; Hsu, M. F.; Nikolaides, M. G.; Marquez, M.; Bausch, A. R.; Weitz, D. A. *Science* **2002**, *298*, 1006.
(14) Hosono, E.; Fujihara, S.; Kakiuchi, K.; Imai, H. *J. Am. Chem. Soc.* **2004**, *126*, 7790.
(15) Liu, B.; Zeng, H. C. *J. Am. Chem. Soc.* **2004**, *126*, 8124.
(16) Yu, D. B.; Yam, V. W. W. *J. Am. Chem. Soc.* **2004**, *126*, 13200.
(17) Yang, Y.; Nogami, M.; Shi, J. L.; Chen, H. R.; Ma, G. H.; Tang, S. H. *Appl. Phys. Lett.* **2006**, *88*, 081110.
(18) Hwang, D. K.; Kang, S. H.; Lim, J. H.; Yang, E. J.; Oh, J. Y.; Yang, J. H.; Park, S. J. *Appl. Phys. Lett.* **2005**, *86*, 222101.

10.1021/ic7008978 CCC: $37.00
Published on Web 08/24/2007

on. Various nanostructures of ZnO, such as nanobelts, nanocombs, nanosprings, nanohelix, nanobridges, nanonails, and nanocables have already been synthesized by a variety of methods, including thermal evaporation, chemical vapor deposition (CVD), electrodeposition, and template-directed growth.[21−29] Because of its importance in many fields of technology, a number of hollow ZnO nanostructures have been prepared, which include asymmetric hollow nanoarchitectures,[30] hourglass-like nanostructures,[31] and hollow microhemispheres.[32] However, it still remains a challenge to identify a facile and suitable method for growing high-quality in terms of monodisperse and well-shaped hollow ZnO nanostructures.

Herein, we report the fabrication of hexagonal ZnO microprisms with regular interior space by a facile template-free method. The structure and morphology can be controlled easily. The first step, experimentally, involved the fabrication of a flower-like hierarchical precursor with the formula of $ZnO{\cdot}0.33ZnBr_2{\cdot}1.74H_2O$, according to our previous report.[33] Because of the low solubility of the precursor in diluted ammonium solution, a controllable release of zinc cations may make the conversion from the precursor to final hollow ZnO nanostructures feasible. To get perfect crystallinity, hydrothermal treatment was adopted to obtain ZnO nanostructure through the reaction of the precursors with ammonia. Interestingly, the hollow hexagonal ZnO microprisms twinned crystallites with (001) as the twinning plane were observed in the typical synthesis. Then, the morphology evolution of the hollow ZnO microprism was investigated by field emission scanning electron microscopy (FE-SEM) and transmission electron microscopy (TEM). In addition, a two-step growth mechanism was revealed: nucleation-growth and preferential chemical dissolution of the metastable faces of the ZnO twinning microcrystal.

Experimental Section

Preparation. Flower-like precursor $ZnO{\cdot}0.33ZnBr_2{\cdot}1.74H_2O$ was first prepared according to our previous work,[33] on the basis of a reverse microemulsion method. ZnO hexagonal microprisms with a hollow nanostructure were synthesized by the hydrothermal reaction of the precursors in an ammonia aqueous solution at suitable temperatures. In a typical experiment, 0.007 g of the precursor was dispersed in 10 mL of 1.04 mol/L diluted ammonia aqueous solution at room temperature, again with ultrasonication for 10 min. Then, the mixture was transferred into a 15 mL Teflon-lined stainless steel autoclave and maintained at 130 °C for 12 h. The white suspension was centrifuged to separate the precipitate, rinsed three times with distilled water, and finally dried in a vacuum oven at 60 °C for 6 h.

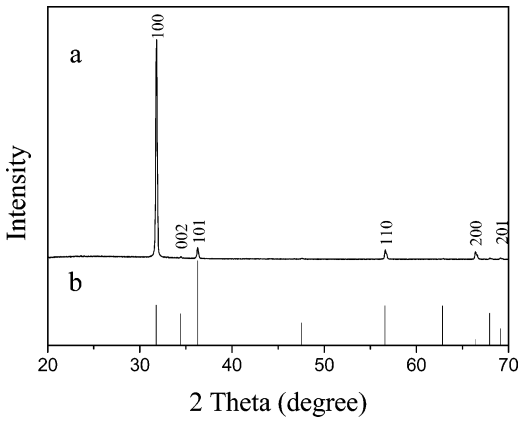

Figure 1. (a) XRD patterns of the hexagonal ZnO hollow microprism and (b) standard ZnO (JCPDS 36−1451).

Characterization. The product was characterized by X-ray diffraction (XRD) using a Rigaku-D/max 2500V X-ray diffractometer equipped with Cu Kα radiation ($\lambda = 1.54178$ Å) at a step width of 0.02°. The morphologies and structures of the as-synthesized ZnO products were characterized by field emission scanning electron microscopy (FE-SEM) and transmission electron microscopy (TEM). All of the samples for the FE-SEM and TEM characterization were prepared by directly transferring the suspended products to the ITO glass slide and the standard copper grid coated with an amorphous carbon film, respectively. FE-SEM analysis was performed on a Philips XL-30 field-emission scanning electron microscope operated at 15 kV, while TEM and selected area electron diffraction (SAED) were carried out on a JEOL-JEM-2010 at 200 kV. The PL spectrum of the ZnO sample was measured on a Hitachi 4500 fluorescence spectrophotometer using a xenon lamp as an excitation source, with an excitation wavelength of 325 nm at room temperature.

Results and Discussion

Structure and Morphology. Part a of Figure 1 shows the XRD pattern of the as-synthesized hexagonal hollow microprism. All of the reflection peaks of the ZnO samples can be indexed as pure hexagonal ZnO (JCPDS card number 36−1451). Compared with the standard diffraction pattern (part b of Figure 1), the deviation of peak intensities implies the preferential chemical partial dissolution of the metastable (001) plane, which is consistent with what was reported in the literature.[34−36] Typical morphology of the as-synthesized ZnO hollow nanostructures are presented in Figure 2. From the SEM pictures of typical ZnO nanostructure (part a of

(19) Tang, Z. K.; Wong, G. K. L.; Yu, P.; Kawasaki, M.; Ohtomo, A.; Koinuma, H.; Segawa, Y. *Appl. Phys. Lett.* **1998**, *72*, 3270.
(20) Rensmo, H.; Keis, K.; Lindström, H.; Södergren, S.; Solbrand, A.; Hagfeldt, A.; Lindquist, S. E.; Wang, L. N.; Muhammed, M. *J. Phys. Chem. B* **1997**, *101*, 2598.
(21) Pan, Z. W.; Dai, Z. R.; Wang, Z. L. *Science* **2001**, *291*, 1947.
(22) Cheng, B.; Shi, W. S.; Russell-Tanner, J. M.; Zhang, L.; Samulski, E. T. *Inorg. Chem.* ***2006***, *45*, *1208*.
(23) Kong, X. Y.; Wang, Z. L. *Nano Lett.* **2003**, *3*, 1265.
(24) Gao, P. X.; Wang, Z. L. *J. Am. Chem. Soc.* **2003**, *125*, 11299.
(25) Lao, J. Y.; Wen, J. G.; Ren, Z. F. *Nano Lett.* **2002**, *2*, 1287.
(26) Choi, K. S.; Lichtenegger, H. C.; Stucky, G. D. *J. Am. Chem. Soc.* **2002**, *124*, 12402.
(27) Liu, C. H.; Zapien, J. A.; Yao, Y.; Meng, X. M.; Lee, C. S.; Fan, S. S.; Lifshitz, Y.; Lee, S. T. *Adv. Mater.* **2003**, *15*, 838.
(28) Lao, J. Y.; Huang, J. Y.; Wang, D. Z.; Ren, Z. F. *Nano Lett.* **2003**, *3*, 235.
(29) Wu, J. J.; Liu, S. C.; Wu, C. T.; Chen, K. H.; Chen, L. C. *Appl. Phys. Lett.* **2002**, *81*, 1312.
(30) Yao, K. X.; Zeng, H. C. *J. Phys. Chem. B* **2006**, *110*, 14736.
(31) Yao, K. X.; Sinclair, R.; Zeng, H. C. *J. Phys. Chem. C* **2007**, *111*, 2032.
(32) Mo, M. S.; Yu, J. C.; Zhang, L. Z.; Li, S. A. *Adv. Mater.* **2005**, *17*, 756.
(33) Yu, S. Y.; Wang, C.; Yu, J. B.; Shi, W. D.; Deng, R. P.; Zhang, H. J. *Nanotechnology* **2006**, *17*, 3607.
(34) Hu, J. Q.; Bando, Y. *Appl. Phys. Lett.* **2003**, *82*, 1401.
(35) Jeong, J. S.; Lee, J. Y.; Cho, J. H.; Suh, H. J.; Lee, C. J. *Chem. Mater.* **2005**, *17*, 2752.
(36) Vayssieres, L.; Keis, K.; Hagfeldt, A.; Lindquist, S. T. *Chem. Mater.* **2001**, *13*, 4395.

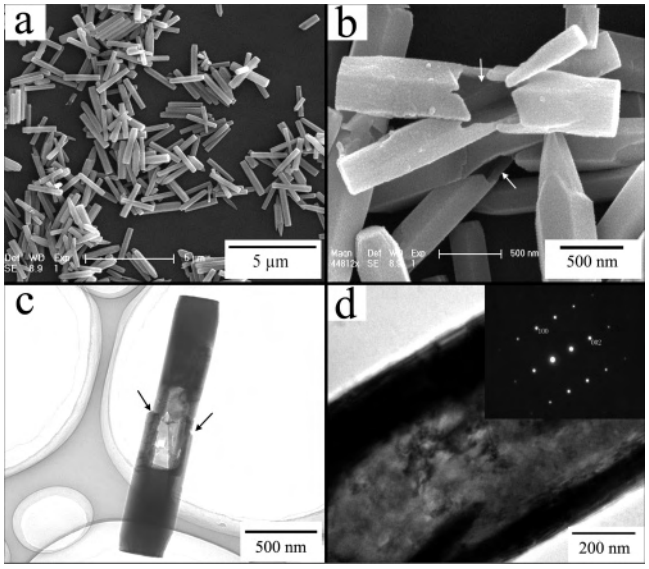

Figure 2. (a) Low-magnification and (b) high-magnification FE-SEM images of the typical hexagonal ZnO microprism with hollow nanostructures, (c) TEM image of a single hollow ZnO microprism, (d) high-magnification TEM image of the central section of a typical hexagonal ZnO microprism with hollow nanostructures (inset, SAED pattern).

Figure 2), it is clear that microprisms with closed-end and regular hexagonal sections are the dominant products. The detailed morphology of hollow nanostructures can be seen under higher magnification in part b of Figure 2. The well-faceted hollow particles have a diameter of about 500 nm and a length of up to 2−3 μm (part b of Figure 2). Hollow interior space can be observed clearly from some fractured hollow microprisms, as a result of ultrasonication and washing in the process of the experiment (indicated with white arrows). The interior shell of the fragment is smooth and about 40−50 nm in thickness. The morphology and structure of typical samples observed from SEM images are in line with what is viewed from TEM images in parts c and d of Figure 2. In part c of Figure 2, it can be seen that the microprism has two solid ends and regular interior space. It is interesting to note that the crystallite of the ZnO hollow microprism is symmetrical about a twinning plane (indicated with black arrows in part c of Figure 2). A high-magnification TEM image of hollow ZnO nanostructures (part d of Figure 2) shows the central section of the microprism has a less compact surface where the crystallites of the lamella shell can be observed. Confirmed with the corresponding SAED pattern recorded from the nanostructures in part d of Figure 2, the individual elongated ZnO crystallites are single-crystalline with their axes pointing along [001] of the crystal.

Effect of Reaction Conditions on the Growth of ZnO Nanostructure. Generally, several parameters were identified as important factors in controlling the size, morphology, and homogeneity of the ZnO nanostructure, namely the reaction temperature, the concentration of ammonia aqueous solution, and the nature of the solvent. By changing these parameters, we got a series of ZnO nanostructures whose morphologies are shown in Figures S1−S3 (Supporting Information), respectively. Figure S1 exhibits low-magnification and high-magnification FE-SEM images of products obtained at 150, 160, 180, and 200 °C, respectively, on the basis of the standard conditions. By altering the reaction temperature, it can be seen that the shape of the ZnO nanostructure changes nothing, yet the size and homogeneity vary much. In addition, it can be observed that different morphologies were obtained under the standard conditions by changing the concentration of ammonia aqueous solution from 0.27 to 1.27 mol/L (Figure S2). The decrease of the concentration of the ammonia aqueous solution led to spindle-like microrods with a diameter of 500 nm (parts a and b of Figure S2). When the concentration of the ammonia aqueous solution is lower than 0.54mol/L, no hollow structure can be observed. High concentrations of ammonia aqueous solution, such as 1.27mol/L, will destroy the integrality of structure because of the fracture of shell at the central section (part d of Figure S2). Appropriate concentration of the ammonia aqueous solution is favorable for the growth of the perfect hollow structure. In such a system, the hollow ZnO microprism can only be obtained when the concentration of ammonia is controlled in the range of 0.79−1.04 mol/L (part c of Figure S2). To show the effect of the solvent on the ZnO morphology, we applied mixed solvents (ethanol and distilled water) instead of distilled water. Figure S3 shows the SEM images of the sample obtained in a mixed solvent of distilled water and ethanol with different volume ratios. It is clear that the hollow microprism structure formed with a high volume ratio of distilled water and ethanol (V_W/V_E = 4:1) (part d of Figure S3), whereas the rotor-like particles were obtained when the volume ratios are 1:4 and 2:3 (parts a and b of Figures S3), respectively. When the volume ratio is 3:2, a rod-like ZnO nanostructure was obtained (part c of Figure S3). Therefore, it may be concluded that the componential increase of ethanol in the mixed solvent may tend to the second nucleation, whereas the componential increase of distilled water will possibly incline to the growth of hollow microprism. It appears from this study that the influence of mixed solvents, the concentration of ammonia aqueous solution, and the reaction temperature on the morphology is complex. More detailed investigations for the effects of these parameters on the ZnO nanostructures are in progress.

Studies of the Growth Process. To understand the growth mechanism, the growth process was also monitored by time-dependent observations. Figure 3 shows the SEM and TEM images of the products that were obtained at 130 °C after heating for 2, 6, 12, and 24 h. Part a of Figure 3 reveals that grenade-like hexagonal microprisms (indicated with black arrows) with the bottom subunit much larger than the top subunit could be obtained at the initial reaction stage, for example at 2 h. The bottom subunit was ∼200−500 nm in width and ∼500−800 nm in length, whereas the top subunit was ∼100−200 nm wide and ∼200−300 nm long. This typical morphology of twinning ZnO has been reported in the previous literature.[37−41] After a hydrothermal treatment

(37) Boyle, D. S.; Govender, K.; O'Brien, P. *Chem. Commun*. **2002**, 80.
(38) Govender, K.; Boyle, D. S.; Kenway, P. B.; O'Brien, P. *J. Mater. Chem.* **2004**, *14*, 2575.
(39) Tang, J.; Cui, X. Q.; Liu, Y.; Yang, X. R. *J. Phys. Chem. B* **2005**, *109*, 22244.

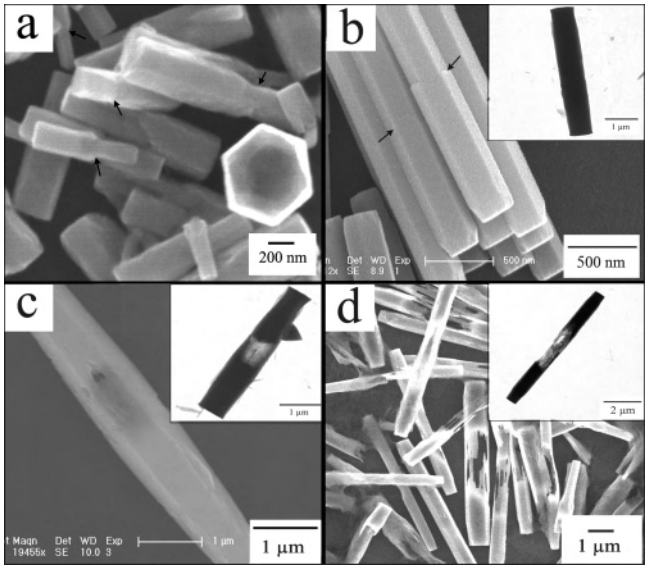

Figure 3. FE-SEM images of the obtained ZnO products for different times: (a) 2 h, (b) 6 h, (c) 12 h, and (d) 24 h. (Inset, enlarged images of particles in parts b, c, and d).

of over 6 h, faceted and hexagonal ZnO microprisms were obtained with ~400−600 nm in width and ~1.5−2 μm in length. The microparticles grew thicker and longer and showed better crystal perfection. The smaller subunit of the twinning evolved to be equivalent to the bigger one, and the two subunits were symmetrical about the twinning plane. It is worth noting that, however, there are still lots of defects in the rougher surface at the central section of particle (indicated with black arrows in part b of Figure 3), where the two subunits fuse together. When the reaction time was extended to 12 h, well-faceted ZnO microprisms with interior space at the central section of microparticles appeared, as seen in part c of Figure 3. As the aging process was extended to 24 h, the length/diameter ratio of the particles increased, and the shell of hollow parts grew more frangible, leading to the breaking up of the central section of most of the microprisms (part d of Figure 3).

To comprehend the possibility of generating ZnO hollow microprisms, one has to understand its structural characteristics. From its anisotropic structure, ZnO can be described as many alternating planes composed of tetrahedral coordinated O^{2-} and Zn^{2+} ions, the growth units ZnO_4^{6-} ions, stacked alternately along the *c* axis. The oppositely charged ions produce (001) and (00$\bar{1}$) polar surfaces.[42] Consequently, the most stable growth habit of the ZnO crystal is to elongate along the *c* axis.

With regard to the forming mechanism of the ZnO twinning crystal, a few models can be suggested. Wang et al. found that the linkage of ZnO_4^{6-} tetrahedral units in a weak basic solution leads to the formation of a crystal nucleus of a twinning crystal.[43] When this kind of crystal

Scheme 1. Schematic Illustration of the Formation Process of Typical Hexagonal ZnO Microprisms with Hollow Nanostructures[a]

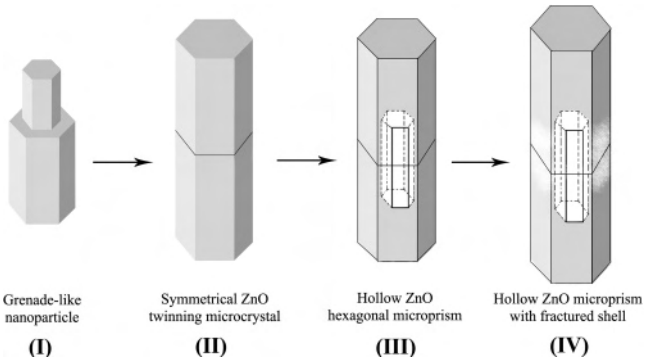

[a] (I) Grenade-like asymmetrical ZnO twinning microcrystal, (II) formation of symmetrical ZnO twinning microprism with legible grain boundary, (III) faceted and hexagonal ZnO microprisms with regular interior space, and (IV) hollow ZnO microprisms with a fractured shell.

nucleus exists in solution, the growth of the individual crystallite in the twins would take place along the polar *c* axis by the incorporation of growth units on the growth interfaces, such as (001), and thus twinned crystallites can finally be formed. It may be energetically favorable to joint the polar surfaces with higher energy, to lower the system energy in such experimental conditions.

On the basis of the experimental results in our case and our understanding of the process, a proposed growth mechanism for hollow ZnO nanostructures is given in Scheme 1. First, the precursors partially dissolved and reacted with ammonia aqueous solution to form $[Zn(OH)_n(NH_3)_m]^{2-n}$. Then, the intermediate product rapidly decomposed and grew into grenade-like ZnO asymmetrical twinning crystals. As the reaction time increased, the microprisms grew thicker and longer and became symmetrical about the twinning plane. The surface of central section was still coarse, where the density of the defects is highest. In the previous report,[36] the preferential chemical dissolution of the metastable (001)-Zn faces of the oriented microrods would take place and lead to the required oriented hollow structure in the aging process. The energy of hollow structure may be lower than that of the solid structure as a result of the higher energy at the polar surfaces.[44] Consequently, when the aging time was extended, the dissolution with a higher rate would carry out on the interface of two twinning subunits in our system. Through penetrating at the defect sites of the coarse shell, preferential dissolution of the twinning (001) plane may result in a hollow structure with regular interior space. On the other hand, growth along the *c* axis was synchronous with the dissolution of the (001)-Zn faces. Then, the systems may tend to reach their thermodynamic equilibrium and result in a typical hollow morphology, as a result of the aging mechanism of Ostwald ripening.[45] If the aging time is sufficient, a high dissolution rate may lead to the fracture of the shell at the central section, where the density of the defects is highest.

(40) Vanheusden, K.; Seager, C. H.; Warren, W. L.; Tallant, D. R.; Voigt, J. A. *Appl. Phys. Lett.* **1996**, *68*, 403.
(41) Yu, Q. J.; Yu, C. L.; Yang, H. B.; Fu, W. Y.; Chang, L. X.; Xu, J.; Wei, R. H.; Li, H. D.; Zhu, H. Y.; Li, M. H.; Zou G. T.; Wang, G. R.; Shao, C. L.; Liu Y. C. *Inorg. Chem.* **2007**, ASAP.
(42) Li, F.; Ding, Y.; Gao, P. X.; Xin, X. Q.; Wang Z. L. *Angew. Chem., Int. Ed.* **2004**, *43*, 5238.
(43) Wang, B. G.; Shi, E. W.; Zhong W. Z. *Cryst. Res. Technol.* **1998**, *33*, 937.
(44) Yu, H.; Zhang, Z.; Han, M.; Hao, X.; Zhu, F. *J. Am. Chem. Soc.* **2005**, *127*, 2378.
(45) Liu, B.; Zeng, H. C. *Langmuir* **2004**, *20*, 4196.

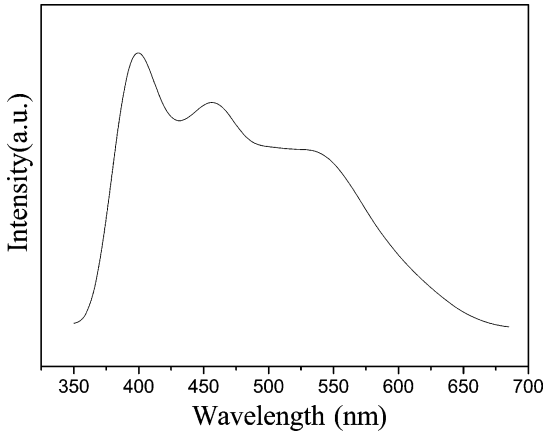

Figure 4. Room-temperature PL spectrum of a typical hexagonal hollow ZnO nanostructure. (λ_{ex} = 325 nm).

Optical Properties. The PL spectrum of the ZnO hollow microprisms was measured with the excitation wavelength of 325 nm at room temperature (Figure 4). The spectrum of the ZnO hollow nanostructure consists of three emission bands: the ultraviolet emission at around 400 nm, the blue band (~457 nm), and the green band (~540 nm). The UV emission could be attributed to the near band-edge emission of the intrinsic wide band gap of ZnO, resulting from the recombination of excitonic centers.[46] The green PL is assigned to the recombination of photoexcited electrons with deeply trapped holes in the singly ionized oxygen vacancy.[47,48] The visible emission is usually considered to be related to various intrinsic defects produced during ZnO preparation and post-treatment.[49,50] In previous work, the blue-band emission from ZnO was also reported. Unfortunately, the exact origins have not been assigned so far.[51,52] Therefore, further studies from both theoretical and experimental perspectives on the PL properties of such ZnO nanostructures are required to reveal the underlined photoluminescence mechanisms.

Conclusion

To conclude, we have demonstrated that hexagonal ZnO microprisms with hollow architecture can be fabricated with large-scale yield via a template-free hydrothermal synthetic route. Furthermore, the possible growth mechanism of the hollow structure has been analyzed via a time-dependent observation. The morphologies of products depend on the experimental conditions such as the solvent, the concentration of ammonia aqueous solution, and the reaction temperature. The formation of such hollow nanostructures is believed to be the result of the preferential dissolution of the metastable (001)-Zn faces of the twinned microprisms from the defect sites on the twinning plane. This type of hollow nanoarchitecture shows unique PL characteristics, which might be potentially useful material in future optoelectronic applications.

Acknowledgment. The authors are grateful for financial aid from the National Natural Science Foundation of China (Grants 20490210, 206301040, and 20602035) and the MOST of China (Grants 2006CB601103 and 2006DFA42610).

Supporting Information Available: SEM images. This material is available free of charge via the Internet at http://pubs.acs.org.

IC7008978

(46) Huang, M. H.; Wu, Y. Y.; Feick, H. N.; Tran, N.; Weber, E.; Yang, P. D. *Adv. Mater.* **2001**, *13*, 113.
(47) Vanheusden, K.; Warren, W. L.; Seager, C. H.; Tallant, D. R.; Voigt, J. A.; Gnade, B. E. *J. Appl. Phys.* **1996**, *79*, 7983.
(48) Özgür, Ü.; Alivov, Ya. I.; Liu, C.; Teke, A.; Reshchikov, M. A.; Doğan, S.; Avrutin, V.; Cho, S. J.; Morkoç, H. *J. Appl. Phys.* **2005**, *98*, 041301.
(49) Hsu, N. E.; Hung, W. K.; Chen, Y. F. *J. Appl Phys.* **2004**, *96*, 4671.
(50) Li, D.; Leung, Y. H.; Djurisic, A. B.; Liu, Z. T.; Xie, M. H.; Shi, S. L.; Xu, S. J.; Chan, W. K. *Appl. Phys. Lett.* **2004**, *85*, 1601.
(51) Fu, Z. X.; Lin, B. X.; Liao, G. H.; Wu, Z. Q. *J. Cryst. Growth* **1998**, *193*, 316.
(52) Jiang, C. L.; Zhang, W. Q.; Zou, G. F.; Yu, W. C.; Qian, Y. T. *J. Phys. Chem. B* **2005**, *109*, 1361.